

Boundary-Condition-Independent Reduced-Order Modeling of Complex 2D Objects by POD-Galerkin Methodology

Arun Prakash Raghupathy, Urmila Ghia, Karman Ghia
Computational Fluid Dynamics Research Laboratory
University of Cincinnati, Cincinnati, OH 45221
raghupa@email.uc.edu

William Maltz
Electronic Cooling Solutions Inc
Mountain View, CA 95134
wmaltz@ecooling.com

Abstract

The objective of the current work is to introduce the concept of boundary-condition-independent (BCI) reduced-order modeling (ROM) for complex electronic packages by the POD-Galerkin methodology. Detailed models of complex electronic packages are used within system-level models in Computational Fluid Dynamics (CFD)-based heat transfer analysis. At times, these package-level models are complicated, and their simulation tends to consume large amounts of computational resources. This problem is compounded further if multiple instances of these models are used within the system. If a package-level model that reduces computational resources (reduced-order model), and provides results in many different flow situations (boundary-condition-independent model) can be deployed, it will accelerate the design and analysis of the end products that make use of these components. This work focuses on how the Proper Orthogonal Decomposition (POD)-Galerkin methodology can be used with the Finite Volume (FV) method to generate reduced-order models that are boundary-condition-independent. This method is successfully used in the present study to generate boundary-condition-independent reduced-order models for 1D and 2D objects. Successful implementation of the method is also shown on 2D objects made of multiple materials and multiple heat generating sources. Also, the final BCI ROM in each case is found to work extremely well (errors less than 1%) even for boundary conditions outside the range in which it was generated, making it a truly boundary-condition-independent model.

Keywords

POD, Galerkin, Compact Thermal Model, Boundary-Condition Independent Models

1. Introduction

Network-based Compact Thermal Models (CTMs) were introduced by the DELPHI (DEvelopment of Libraries of PHysical models for an Integrated design environment) project [1, 2] for accurate package characterization and to replace computationally intensive detailed CFD package-level models. This project created a revolution in the field of model development for thermal analysis of electronic packages. To overcome the limitations of the DELPHI method, such as

inability in modeling packages with multiple heat sources and inability in predicting tangential gradients in temperature, alternate approaches [3, 4, 5] have been proposed. These approaches cannot be directly interfaced with CFD software that is currently used in the electronics cooling industry. The present work addresses this issue by demonstrating the use of the POD-Galerkin methodology for developing BCI ROMs.

Shapiro [6] suggested the application of POD to develop reduced-order models of complex electronic systems. He has employed a “reduce-and-interconnect” in his work [6, 7], where reduced-order models for components are generated independently, and then connected using a frequency-response approach. Further application of POD-Galerkin approach in the area of electronics cooling can also be found in the work of Rambo [8]. However, a review of the literature shows limited application of POD along with commercial software for heat transfer analysis. On this front, most of the work [9, 10] involves integration with the Finite Element Method (FEM) as it is commonly used for heat conduction analysis. Also, FEM-based commercial software allows easy access to the mass and stiffness matrices which are used for generating the reduced-order model. Currently, software used in the electronics cooling industry is based on FV solvers. Therefore, it is important to identify methods that can be easily implemented in the existing codes with minimal modifications or by the addition of user-defined subroutines. The work by Astrid [11] addresses the issue of integrating the POD-Galerkin methodology with FV method, and hence, forms the basis for the proposed methodology. The present work identifies POD-Galerkin as a viable technique to generate boundary-condition independent reduced-order models for complex packages.

2. POD-Galerkin Methodology

Introduction to reduced-order modeling using POD-Galerkin methodology is available in the work of Ghia [12] and Shirooni [13] where this method is employed to generate reduced-order models of turbulent flow in an axisymmetric combustor. Also, detailed introductions are available in the work of Rambo [8], Astrid [11] and Atwell [15].

POD is a statistical method of examining the characteristics of a particular data set. Projection of the governing equations onto a subspace, that defines the

characteristics of the data, creates the reduced-order model. The application of POD to obtain a reduced-order model for the transient heat equation is discussed in detail by Astrid [11], and is summarized here in the following steps:

Step 1: A complete relevant data set is constructed. This is achieved by constructing a matrix composed of “snapshots” of the solution over time. For example, the matrix of snapshots, T_{snap} , for the 1D transient heat equation is shown below:

$$T_{snap} = \begin{bmatrix} T(1, timenititl) & \dots & T(1, Notimestep) \\ \vdots & \ddots & \vdots \\ T(No.gridpans, timenititl) & \dots & T(No.gridpans, Notimestep) \end{bmatrix} \quad (1)$$

For the 2D case, the same structure as that of “ T_{snap} ” matrix is used.

Step 2: The covariance matrix is calculated as

$$C = \frac{1}{No} T_{snap} T_{snap}^T \quad (2)$$

where ‘No’ is the number of time steps.

Step 3: Singular-Value-Decomposition of C is performed to identify the eigenvalues and their corresponding eigenvectors.

Step 4: Few of the largest eigenvalues and their corresponding eigenvectors (ϕ_i) are selected and arranged in a matrix. This matrix forms the POD basis (Φ), which is the required subspace.

Step 5: The governing equation is formulated in the discrete form. For the 1D case, the equation is:

$$\rho c_p \frac{\partial T}{\partial t} = k \frac{\partial^2 T}{\partial x^2} \quad (3)$$

Equation 3 is discretized by the fully implicit method for reasons of stability; the method is unconditionally stable. The discretized form is as below:

$$A T(t + \Delta t) = A^0 T(t) + B u(t) \quad (4)$$

Coefficients of the unknown solution are grouped together in the “A” matrix and those of the known temperatures are grouped in the “A⁰” matrix. Sources or information on the boundary conditions is stored in the “B” matrix. Coefficient matrices hold information on the geometry and material properties. The ‘A’ matrix is a sparse matrix consisting of three diagonals for the 1D case and five diagonals for the 2D case.

Step 6: Governing equation in the discrete form is now projected onto the subspace, Φ , by Galerkin projection. The Galerkin projection yields:

$$\Phi^T A \Phi a(t + \Delta t) = \Phi^T A^0 \Phi a(t) + \Phi^T B u(t) \quad (5)$$

Equation 5 is the reduced-order model of the heat equation.

Step 7: The solution is now represented by

$$T(x, t) = \sum_{i=1}^n a_i(t) \phi_i(x) \quad (6)$$

where a_i s are the POD coefficients, and ϕ_i s are the orthonormal POD basis vectors. The reduced-order model governs the evolution of the POD coefficients. The POD coefficients are determined by solving the following equation.

$$a_i(t) = \phi_i^T T(x, t) \quad (7)$$

The number of POD coefficients is of the order of the number of the chosen POD basis vectors. Thus, computation of the solution T on a number of grid points is now reduced to computing the evolution of a few POD coefficients. This provides a reduction in the amount of calculation, while the accuracy of the calculated solution variable is maintained at a high level because the ϕ_i s contain maximum information on the heat transfer process in the 1D or 2D object.

Step 8: The important contribution of the current work is to show that a BCI ROM can be obtained for complex objects using the above methodology. It is possible to obtain such a model by applying the principle of superposition of select boundary conditions. By appending solutions of different types of boundary conditions, the snapshot matrix is constructed.

The snapshot matrix for a BCI ROM is of the form:

$$T_{snap} = \left[T_{BC1} \quad T_{BC2} \quad \dots \quad T_{BCn} \right] \quad (8)$$

where T_{BC} is a solution matrix of size P x Q, P is the number of grid points and Q is the number of time steps. Since transient solutions capture a majority of the characteristics of the object, transient solutions of select boundary conditions are used in the construction of the snapshot matrix. The absolute necessity of using transient solutions for snapshots was also determined during the course of this research. Also, since the method is based on the behavior of solutions, non-linearity in material properties can also be captured and modeled.

3. Error Analysis

In order to understand performance of the BCI ROM, it is necessary to determine all the relevant errors. The BCI ROM that is generated can have two main types of errors.

The first type of error results from using inappropriate boundary conditions to generate the snapshot matrix. Once the reduced-order model is generated, if it does not produce an accurate solution even with reasonable number of POD basis vectors, then the error lies in the construction of the snapshot matrix. On increasing the number of POD basis vectors, the error will not decrease in magnitude; instead it reaches a plateau. If this happens, the error is reduced by modifying the snapshot matrix with appropriate solutions for the snapshot matrix.

The second type of error results from insufficient number of POD basis vectors. The number of POD basis vectors is determined by analyzing the spectrum of eigenvalues and selecting the ones which are of order 0.1 and higher. The following heuristic approach cannot be used as a hard rule for judging the number of POD basis vectors for the BCI ROM.

$$\sum_{i=1}^n \lambda_i / \sum_{i=1}^N \lambda_N \approx 1 \quad (9)$$

where λ is the eigenvalue, n is the selected number of eigenvalues and N is the total number of eigenvalues. Equation (9) does not show how close to 1 should the ratio be.

The smaller eigenvalues hold information like temperature gradient in corners, variations in the initial time step, etc. Error plots and the obtained solution are used as guidelines to select the right number of POD basis vectors. By increasing the number of POD basis vectors, the amount of error continues to decrease. This decrease in error occurs only when the right snapshot matrix is used for developing the BCI ROM. An important observation about the errors obtained from the application of the current methodology is that the error is always unidirectional. The BCI ROM always underpredicts the solution when compared to the solution obtained by CFD. Thus, if the generated reduced-order model has a fixed level of error, a highly accurate final solution can be predicted by addition of this error to the obtained solution.

Errors are analyzed at the initial and final time step by the following relation

$$Error_{timestep} = abs(\max(T_{CFD}(t) - \max(T_{POD}(t))) \quad (9)$$

For a complete perspective over all timesteps, time-averaged error is used and is computed as

$$Error_{time-averaged} = \frac{1}{N} \sum_{t=1}^N (abs(\max(T_{CFD}(t) - \max(T_{POD}(t))_i)) \quad (10)$$

where N is the number of time steps. Both these errors are analyzed in order to understand the performance of the BCI ROM.

4. Results and Discussion

4.1. 1D Object

The methodology and results for the 1D has been discussed in detail in an earlier work [17]. A BCI ROM was generated for a rod with a single heat source at its center, and asymmetric boundary conditions on its ends. The time-averaged error in all cases was found to be less than 1°C (range of 0°C to 100°C). Also, computation of 400 equations was reduced to calculation of 12 equations.

Cases (T_{BC})	Left	Right
1	Ins	0°C
2	Ins	80°C
3	Ins	Ins
4	0°C	Ins
5	80°C	Ins
Validation Case	0°C	0°C
Validation Case	-20°C	200°C

Table 1: Boundary conditions forming the snapshot matrix for the generation of the POD basis vectors for the BCI ROM of the 1D case.

Five snapshots were sufficient to generate a BCI ROM of the heat conduction process in a rod. With a final set of 12

POD basis vectors, heat conduction in a rod with a single heat source can be simulated for any type of boundary condition on its extremities. It was expected that, based on the type of solutions used in the construction of the snapshot matrix, a BCI ROM can be obtained with 9 snapshots for the 2D case, and 13 snapshots for the 3D case. The cases were based on: two snapshots applying extreme boundary conditions for each side, and a single snapshot with insulated boundary condition on all sides. Another important result was establishing the validity of the BCI ROM for boundary conditions outside the range of temperatures used for generating the BCI ROM. The methodology and results obtained for the 1D case requires further investigation before it can be used for complex packages. The sections that follow present the result of this investigation for simple and complex 2D objects.

4.2. 2D Object with a Single Heat Source

Transient conduction is modeled in a copper 2D plate with thermal conductivity $k = 385 \text{ W/m}^2 \text{ K}$, density $\rho = 8930 \text{ kg/m}^3$ and specific heat capacity $c_p = 385 \text{ J/kg K}^{-1}$. The problem configuration is shown in Fig. 1. Number of grid points in the x-direction is 40 and 50 in the y-direction. A heat-generating point source is located at the center of the copper plate. Conduction in the plate is simulated until steady state is reached. Time step size of $\Delta t = 10 \text{ sec}$ is used, and the simulation is performed for 2000 seconds (steady state is reached by this time).

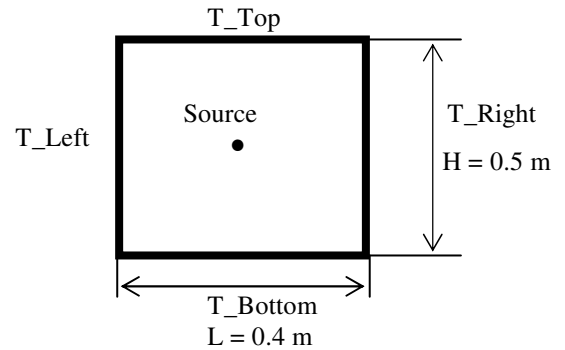


Figure 1: Problem configuration for the 2D case with a single point heat-generating source

Cases (T_{BC})	Boundary			
	Top	Right	Bottom	Left
1	0°C	Ins	Ins	Ins
2	100°C	Ins	Ins	Ins
3	Ins	0°C	Ins	Ins
4	Ins	100°C	Ins	Ins
5	Ins	Ins	0°C	Ins
6	Ins	Ins	100°C	Ins
7	Ins	Ins	Ins	0°C
8	Ins	Ins	Ins	100
9	Ins	Ins	Ins	Ins

Table 2: Boundary conditions forming the snapshot matrix for the generation of the POD basis vectors for the BCI ROM of the 2D case

Validation cases	Boundary			
	Top	Right	South	Left
1	0°C	0°C	0°C	0°C
2	10°C	30°C	5°C	80°C

Table 3: Validation cases for verifying the boundary-condition-independence of the reduced-order model

Based on the conclusions of the 1D case, the snapshot matrix for the 2D object was constructed using the cases in Table 2. Solution for the nine cases is obtained by applying the respective boundary condition to each of the four sides. These solutions are then arranged in the form of the snapshot matrix shown in Eq. (8). Two validation cases, shown in Table 3 are used to prove that the BCI ROM developed can be used to predict solutions for boundary conditions that were not a part of the generating set.

Validation Case 1: A boundary condition of 0°C is applied on all four sides. The reduced-order model is generated with 70 POD basis vectors. The errors at both early ($t = 10s$) and final ($t = 2000s$) timesteps are analyzed. The error at $t=10s$ is in the order of $1e-7^{\circ}C$. The distribution of error in the final time step is shown in Fig. 2. Here it has grown to a maximum of $2.5^{\circ}C$. The time-averaged maximum error is $1.39^{\circ}C$ (for a range of $0^{\circ}C$ to $100^{\circ}C$). Also, the maximum error is observed to occur near the boundary.

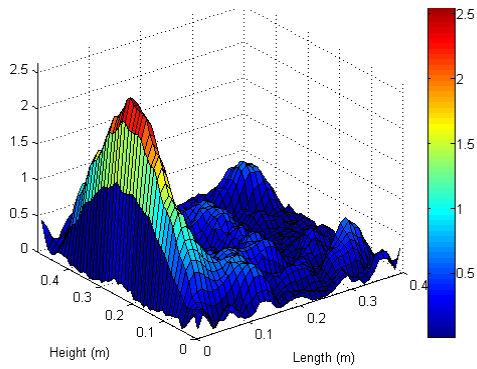
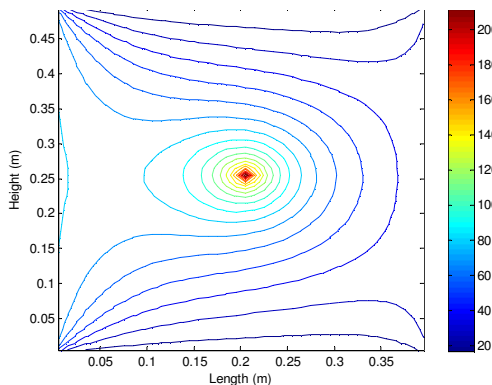
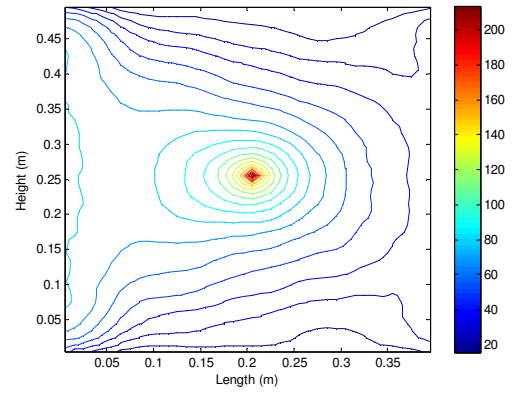


Figure 2: Errors at the final time step over the 2D grid for Validation Case 1



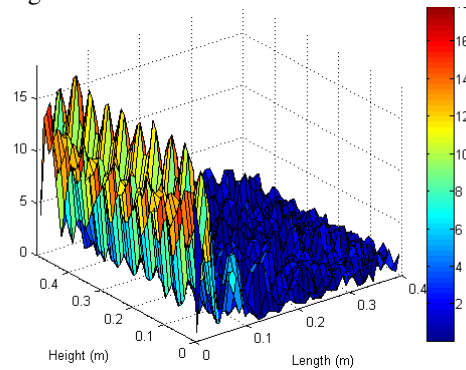
(a) Detailed CFD Model solution



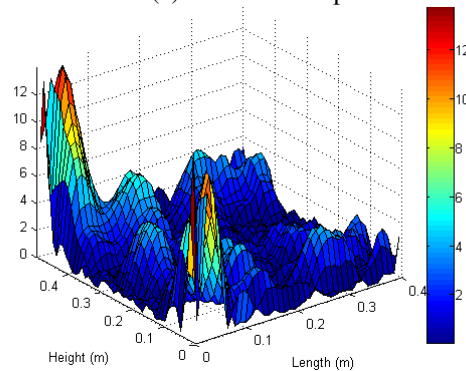
(b) POD solution

Figure 3: Comparison of solution at steady state for validation case 2

Validation Case 2: Second set of boundary conditions shown in Table 3 are applied on the respective sides. These values are arbitrary in nature. Temperatures are chosen in such a way that none of them are equal to the values used in generating the reduced-order model. Also, these temperatures offer strong and weak gradients from the source in the respective directions. It is observed from Figs 3a and 3b that the POD solution at steady state is noticeably different from the CFD solution. The time-averaged maximum error is $14.6^{\circ}C$ (for a range of $0^{\circ}C$ to $100^{\circ}C$). The maximum error during $t = 10s$ is $18^{\circ}C$ and $14^{\circ}C$ at $t = 2000s$. These can be seen in Figs. 4a and 4b.



(a) Initial timestep error



(b) Final timestep error

Figure 4: Errors at various time steps over the 2D grid for Validation Case 2

The high value of errors shows that the BCI ROM is not capturing the dynamics of the transient heat flow in the desired way.

Since this error does not reduce by increasing the number of POD basis vectors, and the maximum error appears close to the boundaries in both validation cases, the fundamental snapshot matrix from which the POD basis is generated has to be revised. The maximum error near the boundary indicates that the BCI ROM is not able to capture strong gradients occurring near boundaries. Therefore in order to capture these gradients, the snapshot matrix is modified to include solutions of cases 10 through 13, shown in Table 4.

The BCI ROM is constructed from 70 POD basis vectors obtained from the revised snapshot matrix. This model is used to predict solution for the two validation cases. Performance of the BCI ROM with different number of POD basis vectors is shown in Table 5 for both validation cases. The errors during the initial and steady state timesteps reduced considerably when higher numbers of POD basis vectors are used. The trend in error shows that the snapshot matrix constructed from cases presented in Table 4 is indeed the right one.

Cases (T _{BC})	Boundary			
	Top	Right	Bottom	Left
1	0°C	Ins	Ins	Ins
2	100°C	Ins	Ins	Ins
3	Ins	0°C	Ins	Ins
4	Ins	100°C	Ins	Ins
5	Ins	Ins	0°C	Ins
6	Ins	Ins	100°C	Ins
7	Ins	Ins	Ins	0°C
8	Ins	Ins	Ins	100°C
9	Ins	Ins	Ins	Ins
10	100°C	0°C	0°C	0°C
11	0°C	100°C	0°C	0°C
12	0°C	0°C	100°C	0°C
13	0°C	0°C	0°C	100°C

Table 4: Boundary conditions forming the revised snapshot matrix for the generation of the POD basis vectors for the BCI ROM of the 2D case.

Validation case	Max Error (°C)	No. of POD Basis vectors		
		70	50	25
1	Initial	0.035	0.350	7.000
	Steady-State	0.006	0.025	0.600
	Time-averaged	0.007	0.054	0.747
2	Initial	0.030	0.800	8.000
	Steady-State	0.018	0.045	1.100
	Time-averaged	0.017	0.059	1.006

Table 5: Errors from the BCI ROM generated using the revised snapshot matrix

Although the error from a BCI ROM constructed from 50 POD basis vectors is less than 1°C, the BCI ROM constructed from 70 POD basis vectors is used because of the expectation that, with strong gradients in unknown boundary conditions, this model will be able to perform better than one constructed using 50 POD basis vectors. Figure 5 shows the POD solution for validation case 2 generated with a BCI ROM constructed using 70 POD basis vectors of the revised snapshot matrix. In comparison with Figs. 3a and 3b, it can be seen that the present solution provides excellent agreement with the solution of the detailed CFD model. In comparison with Fig. 4a, error distribution in Fig. 6 shows a uniform distribution of a low level of error across the 2D object.

Confidence in the boundary-condition-independence of the reduced-order model can only be obtained by employing the reduced-order model for multiple arbitrary boundary conditions. Instead of performing an arbitrary analysis, Taguchi's Design of Experiments (DOE) [18] approach is employed. The Orthogonal Array method uses pair-wise combinations of the independent variables.

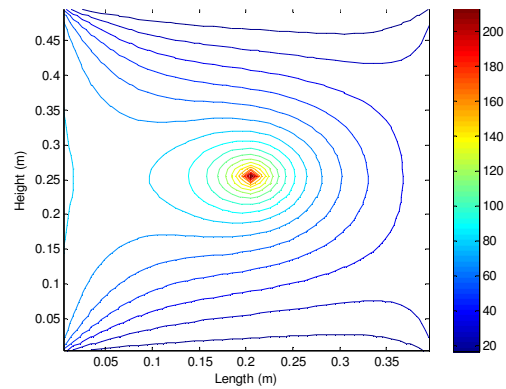


Figure 5: POD Solution from BCI ROM constructed with 70 POD basis vectors of the revised snapshot matrix

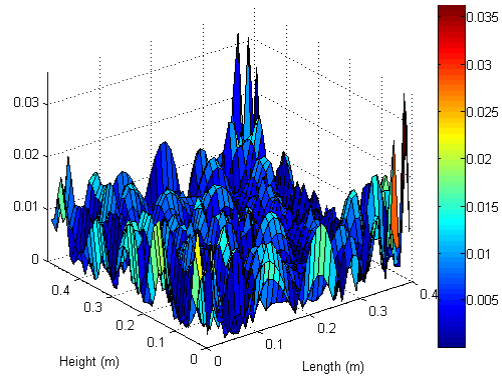


Figure 6: Error distribution at the initial time step for Validation Case 2 obtained from BCI ROM constructed with 70 POD basis vectors of the revised snapshot matrix

The minimum number of experiments to be conducted is given by the following relationship

$$\text{No. of Experiments} = 1 + \sum_{i=1}^M (L_i - 1) \quad (11)$$

where M = No. of independent variables
 L = Level of values the variable can take

Expt. No.	Top (°C)	Right (°C)	Bottom (°C)	Left (°C)
1	25	25	25	25
2	25	50	50	50
3	25	75	75	75
4	50	75	25	50
5	50	25	50	50
6	50	50	75	25
7	75	50	25	75
8	75	75	50	25
9	75	25	75	50

Table 6: L9 Orthogonal Array for verifying boundary-condition-independence of the reduced-order model

The ‘L’ factor is defined by boundary conditions imposed on the reduced-order model. In this case, the L9 Orthogonal Array is used for defining the experiments. The number of factors (4) corresponds to the number of sides. Levels are the temperatures that are applied to the sides. Three temperature levels, namely, 25°C, 50°C and 75°C are used. None of the temperatures used for generating the reduced-order model are used. Table 6 shows the experiments used for validation of the reduced-order model. In all cases, the BCI ROM generated from 70 POD basis vectors of the revised snapshot matrix is used.

Table 7 shows the comparison of the solutions predicted by the BCI ROM against the solutions of the detailed CFD model. The maximum error occurs at lower time steps and is in the order of 0.1 deg C (over a range of 0 to 100°C). Subjecting the BCI ROM to such an experiment provides confidence in the boundary-condition-independence of the reduced-order model.

Expt. No.	Max Error (°C)		
	Initial	Steady-State	Time Averaged
1	0.045	0.003	0.004
2	0.060	0.012	0.016
3	0.090	0.025	0.029
4	0.100	0.016	0.020
5	0.070	0.012	0.015
6	0.090	0.016	0.020
7	0.100	0.020	0.024
8	0.120	0.020	0.025
9	0.090	0.020	0.025

Table 7: Errors from the BCI ROM for the experiments conducted within the temperature range used for generating the reduced-order model

In Table 6, the three levels of temperature (25°C, 50°C and 75°C) used lie within 0 and 100 deg C (extreme values used

while generating the ROM). Table 7 showed that the reduced-order model can indeed be used in an environment that imposes any temperature between 0 and 100 deg C on any side of the 2D object. The nature of reduced-order model generated using POD is such that it captures the characteristics of the data and does not confine itself to any particular boundary condition. The premise that such a reduced-order model should be able to provide accurate results for any boundary condition, even for those that lie outside its generating range, was valid for the 1D case [17]. This is tested again with the 2D object using the DoE approach. Experiments used for testing of this premise are shown in Table 8.

For the experiments in Table 8, the relatively low errors presented in Table 9 show that the reduced-order model generated using the POD-Galerkin method is truly boundary-condition-independent. Although the BCI ROM was generated with insulated cases in its snapshot matrix, it failed to accurately predict certain combinations of insulated and fixed-temperature boundary conditions. By increasing the number of POD basis vectors, those combinations of insulated and fixed-temperature boundary conditions could be predicted with errors of approximately 10%.

Expt. No.	Top (°C)	Right (°C)	Bottom (°C)	Left (°C)
1	-200	-200	-200	-200
2	-200	250	250	250
3	-200	400	400	400
4	250	400	-200	250
5	250	-200	250	250
6	250	250	400	-200
7	400	250	-200	400
8	400	400	250	-200
9	400	-200	400	250

Table 8: L9 Orthogonal Array for verifying truly boundary-condition-independent nature of the reduced-order model

Expt. No.	Max Error (°C)		
	Initial	Steady-State	Time Averaged
1	0.300	0.160	0.150
2	0.250	0.080	0.083
3	0.400	0.160	0.016
4	0.500	0.100	0.113
5	0.220	0.080	0.086
6	0.450	0.100	0.116
7	0.400	0.120	0.138
8	0.600	0.120	0.145
9	0.450	0.040	0.062

Table 9: Errors from the BCI ROM for the experiments conducted outside the temperature range used for generating the reduced-order model

4.3. Complex 2D Object

The concept of BCI ROM is now extended to an object with increased complexity. A reduced-order model is generated for the 2D object shown in Fig. 7. The object has the same dimensions as earlier but now it is constructed from two different materials. Lower half of the 2D plate is made of copper ($k = 385 \text{ W/m}^2\text{K}$, $\rho = 8930 \text{ kg/m}^3$ and $c_p = 385 \text{ J/kgK}^{-1}$) while the upper half is made of aluminum ($k = 201 \text{ W/m}^2\text{K}$, $\rho = 2710 \text{ kg/m}^3$, $c_p = 913 \text{ J/kgK}^{-1}$). The object also has two heat-generating point sources (S1 and S2) of equal strength located asymmetrically. This arrangement of more than one material and multiple sources makes this a complex 2D object. The changes in material properties and the addition of sources are reflected in the co-efficient matrices 'A', 'A0' and 'B' of Eq. (4).

The BCI ROM for the above object is obtained using 70 POD basis vectors generated from the snapshot matrix constructed according to Table 4. This BCI ROM is tested for boundary conditions within the range used for generating the reduced-order model as well as those outside that range. The experiments are discussed in Table 6 and Table 8.

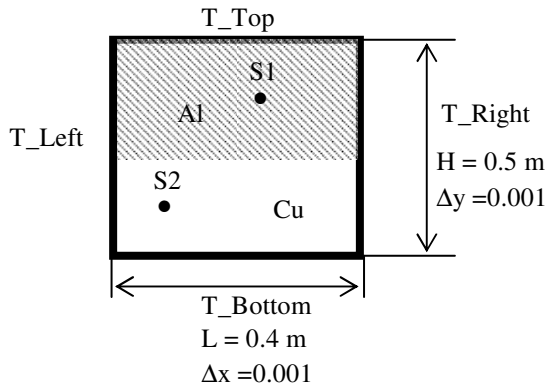


Figure 7: Problem configuration for the 2D case with multiple materials and multiple heat-generating sources

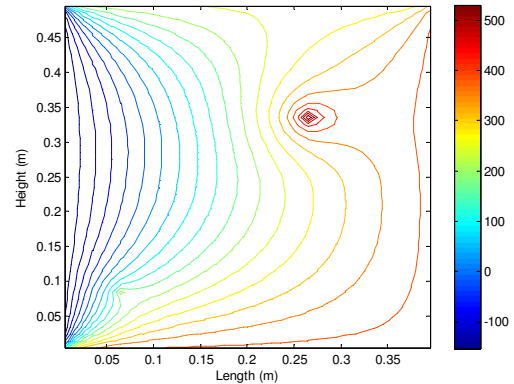
Expt. No.	Max Error ($^{\circ}\text{C}$)		
	Initial	Steady-State	Time Averaged
1	0.040	0.001	0.579
2	0.080	0.080	0.052
3	0.120	0.120	0.103
4	0.090	0.090	0.069
5	0.080	0.080	0.051
6	0.110	0.110	0.069
7	0.120	0.120	0.085
8	0.140	0.140	0.086
9	0.100	0.100	0.085

Table 10: Errors from the BCI ROM for the experiments conducted within the temperature range used for generating the reduced-order model

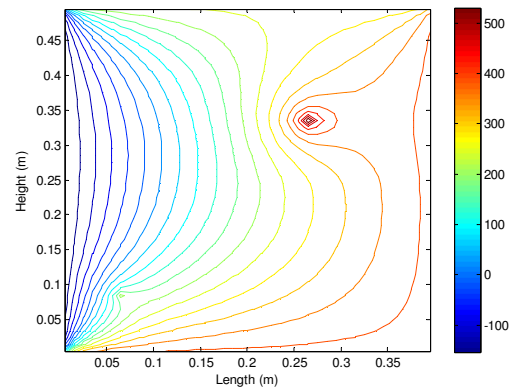
Expt. No.	Max Error ($^{\circ}\text{C}$)		
	Initial	Steady-State	Time Averaged
1	0.250	0.350	0.606
2	0.140	0.350	0.311
3	0.250	0.600	0.615
4	0.180	0.550	0.411
5	0.160	0.550	0.306
6	0.180	0.700	0.412
7	0.200	0.700	0.511
8	0.220	0.900	0.515
9	0.250	0.600	0.506

Table 11: Errors from the BCI ROM for the experiments conducted outside the temperature range used for generating the reduced-order model

Errors corresponding to the experiments in Table 6 are presented in Table 10, and errors corresponding to experiments in Table 8 are shown in Table 11. It can be seen that the errors in all cases are less than 1°C (over a range of -200°C to 400°C). Figures 8a and 8b show good agreement between the results from the detailed CFD model and the BCI ROM. The maximum error, of the order of 0.1°C , between the solutions from the detailed and reduced-order model still occurs only during the final time step.



(a) Detailed CFD Model solution



(b) POD Solution

Figure 8: Comparison of solutions from detailed CFD model and BCI ROM for boundary conditions of Expt. 8 in Table 9

5. Conclusions

The usage of POD-Galerkin methodology to generate BCI ROMs has been successfully demonstrated for both 1D and complex 2D objects. Major advantages of this methodology are as follows:

- It is possible to predict the complete characteristics of the system with a high level of accuracy. Difference between the detailed CFD model and the BCI ROM was always maintained less than 1°C over a range of -200°C to 400°C for the complex 2D object.
- It is possible to obtain large reduction in computational resources and time consumed. This was shown by reducing the computation of 2000 equations to 70 while preserving a high level of accuracy for the complex 2D object.
- The methodology is capable of generating reduced-order models for any complex electronic package with multiple heat-generating sources.
- The methodology is capable of accurately predicting solutions over a wide range of boundary conditions because of the truly boundary-condition independent nature of the obtained reduced-order model.
- The methodology is capable of reliable and accurate prediction of transient solutions
- Also, the methodology, by its nature, is capable of modeling the non-linear characteristics of complex electronic packages

Future efforts will concentrate on extending this methodology to 3D objects and also on interfacing the methodology with existing commercial codes through user-defined functions or macros.

Acknowledgments

The authors acknowledge the support of Electronic Cooling Solutions, Cisco Systems and Avago Technologies, California, for funding this research. Also, communication with Dr. Attila Aranyosi is gratefully acknowledged.

References

1. Lasance, C., Vinke, H., Rosten, H., and Weiner, K.L., 1995, "A Novel Approach for the Thermal Characterization of Electronic Parts", Proc. of SEMITHERM XI, San Jose, CA, pp. 1-9.
2. Lasance, C. J. M., 2008, "Ten Years of Boundary-Condition-Independent Compact Thermal Modeling of Electronic Parts: A Review", Heat Transfer Engineering, Vol. 29, No.2, pp. 149-168.
3. Sabry, M. N., 2007, "Flexible Profile Compact Thermal Models for Practical Geometries" Trans. of the ASME, pp.256-259 Vol. 129.
4. Codecasa, L., D'Amore, D., Maffezzoni, P., and Batty, W., 2002, "Multi-Point Moment Matching Reduction of Distributed Thermal Networks," 8th International Workshop on Thermal Investigation of ICs and Systems, THERMINIC, Madrid, Spain, pp. 231-234.
5. Augustin, A., Hauck, T., Maj, B., Czernohorsky, J., Rudnyi, E.-B., and Korvink, J.-G., 2006, "Model Reduction for Power Electronics Systems with Multiple Heat Sources",

- Proc. of 12th International Workshop on Thermal investigations of ICs, THERMINIC, p. 113-117.
6. Shapiro, B., 2003, "Creating Compact Models of Complex Electronic Systems: An Overview and Suggested Use of Existing Model Reduction and Experimental System Identification Tools", IEEE Trans. on Comp., Parts and Manf. Technology, vol 26, no 1, pg 165-172.
7. Mathai, P., and Shapiro, B., 2006, "Interconnection of Subsystem Reduced Order Models in the Electro-thermal Analysis of a Large System", IEEE Trans. on Components and Packaging Technologies., Vol 30, pp. 317-329.
8. Rambo, J., 2006, "Reduced-order Modeling of Multiscale Turbulent Convection: Application to Data Center Thermal Management", Doctoral Dissertation, Georgia Institute of Technology.
9. Fic, A., Bialecki, R. A., and Kassab, A.J., 2004, "Solving Transient Nonlinear Heat Conduction Problems by Proper Orthogonal Decomposition and FEM", ICHMT International Symposium on Advances in Computational Heat Transfer, Norway, Books of Abstracts, CHT-04-173.
10. Rudnyi, E. B., Lienemann, J., Greiner, A., and Korvink, J.G., 2004, "mor4ansys: Generating Compact Models Directly from ANSYS Models" Technical Proceedings of the 2004 Nanotechnology, Conference and Trade Show, Nanotech 2004, Boston, Massachusetts, USA, vol. 2, p. 279-282, March 7-11.
11. Astrid, P., 2004, "Reduction of Process Simulation Models: A Proper Orthogonal Decomposition Approach", Doctoral Dissertation, Technische Universiteit Eindhoven.
12. Ghia, U., Shirooni, S., Ghia, K., and Osswald, G., 1991, "Examination of a Vortex-Ring Interaction Phenomenon in an Axisymmetric Flow", AIAA-1991-548 Aerospace Sciences Meeting, 29th, Reno, NV.
13. Shirooni, S., 1994, "Analysis of Flow Through Combustor Geometry using Numerical Simulation and Dynamical System Approach", Doctoral Dissertation, University of Cincinnati.
14. Versteeg, H.K., and Malalasekera, W.K., 1995, "An Introduction to Computational Fluid Dynamics, The Finite Volume Method", Pearson Prentice Hall, Essex.
15. Atwell, J. A., 2000, "Proper Orthogonal Decomposition for Reduced Order Control of Partial Differential Equations", Doctoral Dissertation, Virginia Polytechnic Institute and State University.
16. Sirovich L., 1987, "Turbulence and Dynamics of Coherent Structures, Part I: Coherent Structures", Quarterly of Applied Mathematics, XLV:561-571.
17. Raghupathy, A.P., Ghia, U., Ghia, K., and Maltz, W., 2008, "Boundary-Condition-Independent Reduced-Order Modeling of Heat Transfer in Complex Objects by POD-Galerkin Methodology: 1D Case Study", ASME Journal of Heat and Mass Transfer, in review.
18. G. Taguchi and Y. Yokoyama, 1994, "Taguchi Methods: Design of Experiments", American Supplier Institute, Dearborn MI.